water

MDPI

Article

Dynamic Permeability Evolution and Characterization of Cleat-Hydraulic Fractures in Deep Coal Under Stress-Hydrochemical Coupling

Dejiang Li [1,2,3,†], Ze Deng [1,2,3], Yonghui Wu [4,*,†], Caiyuan Dong [1,2,3], Kerui Liu [5], Yan Chang [1,2,3] and Jidong Zhang [1,2,3]

[1] State Key Laboratory of Enhanced Oil and Gas Recovery, Beijing 100083, China; lidejiang69@petrochina.com.cn (D.L.); dengze@petrochina.com.cn (Z.D.); dongcn69@petrochina.com.cn (C.D.); changyan05@petrochina.com.cn (Y.C.); zhangjd69@petrochina.com.cn (J.Z.)
[2] CNPC Key Laboratory of Coal-Rock Gas, Langfang 065007, China
[3] PetroChina Research Institute of Petroleum Exploration & Development, Beijing 100083, China
[4] School of Mines, China University of Mining and Technology, Xuzhou 221116, China
[5] School of Resources and Geosciences, China University of Mining and Technology, Xuzhou 221116, China
* Correspondence: wuyonghuijr@cumt.edu.cn
† These authors contributed equally to this work.

Abstract

The cleat-hydraulic fracture system in deep coal is the main medium controlling the seepage capacity of coal, but under the combined action of high in situ stress and retained fracturing fluid, the permeability of the fracture system is significantly affected by stress and hydrochemical condition. Clarifying the dynamic seepage evolution of coal fractures under stress-hydrochemical coupling is therefore of great significance for optimizing the production schedule and achieving efficient development of deep coalbed methane (CBM) wells. In this study, the No. 8 coal of the Benxi Formation in the Ordos Basin was taken as the research object. Eight standard cylindrical plugs (Φ25 mm × 50 mm) were tested, including four intact samples representing the natural cleat system and four pre-fractured (self-propped) samples representing the cleat-hydraulic fracture system. Overburden helium permeability experiments were conducted at a pore pressure of 1.38 MPa under stepwise confining pressures of 3.45–24.14 MPa along three stress paths (first loading, secondary loading and stepwise unloading). The hydrochemical treatment is realized by soaking the samples in water for 24 h followed by air-drying for 12 h, after which the permeability tests were repeated. Finally, a dynamic permeability model was established on the basis of the experimental results, and the permeability characterization parameters of coal fractures under different conditions were determined. The results show that the permeability of all samples decreases exponentially with increasing confining pressure, and that the fracture type and cleat connectivity dominate the sample permeability. A single directly through-going fracture can increase the initial permeability of intact coal by 5–10 times and markedly reduce its decay rate. A sample with highly developed and well-connected cleats has an initial permeability as high as 32.36×10^{-3} μm^2, i.e., 8–30 times higher than other pre-fractured samples. Secondary loading reduces the permeability at the same confining pressure by 20–40%, and after stress recovery the permeability only rebounds to 35–60% of the first-loading level, indicating that a large part of the fracture closure is irreversible plastic deformation. Hydrochemical treatment can improve fracture connectivity and enhance permeability, and the effect is jointly controlled by the degree of cleat development and mineral filling characteristics. For a sample with well-developed

Check for updates

Academic Editor: Liliana Lefticariu

Received: 13 October 2026
Revised: 30 October 2026
Accepted: 3 November 2026
Published: 5 November 2026

Copyright: © 2026 by the authors. Licensee MDPI, Basel, Switzerland. This article is an open access article distributed under the terms and conditions of the Creative Commons Attribution (CC BY) license.

cleats filled with calcite, the permeability after treatment increases to 2.0–3.7 times the pre-treatment value and the stress sensitivity decreases markedly, indicating that dissolution of the filling calcite reopens and interconnects the originally cemented and sealed cleats and natural fractures, forming more continuous and closure-resistant seepage channels. By fitting the experimental data with the permeability model, the distribution of the fracture stress-sensitivity coefficient under different conditions was obtained. The main limitations of this study are that each test condition was performed on a single specimen without replicate tests, that the water chemistry and dissolved-ion concentrations during soaking were not measured, and that the model parameters were calibrated under specific loading conditions, so caution is required when extrapolating them to reservoir conditions. This study clarifies the dynamic permeability evolution of deep coal fractures and the parameters for predicting the permeability of coal fracture systems, providing an important reference for hydraulic fracturing and the optimized design of production schedules in gas wells.

Keywords: deep coalbed methane; stress-hydrochemical coupling; hydraulic fracture; cleat; dynamic permeability

1. Introduction

CBM occurs in an adsorbed state on the micropore surfaces of the coal matrix, and permeability and gas saturation are the key parameters controlling single-well production [1]. In recent years, with advances in horizontal wells and large-scale volumetric fracturing, CBM exploration has been extending from shallow (<1000 m) to deep (>2000 m) reservoirs. According to an evaluation of 94 major coal-bearing basins worldwide, the geological resources of coal-rock gas in deep coal are about 232×10^{12} m^3, of which Russia, Canada, the USA, China and Australia account for more than 90% [2,3]. In the Ordos Basin, for example, a coal-rock gas well has reached a production of 6×10^4 m^3/d after high-rate, large-scale, multi-stage cluster fracturing [4], demonstrating considerable potential. Fracturing of coal creates a multi-scale network of cleats and hydraulic fractures, which is the core means of enlarging the drainage area and enhancing single-well production [5,6]. However, deep coal reservoirs have long been subjected to a high effective stress environment, complicated further by the hydrochemical treatment caused by fracturing-fluid invasion, and whether their dynamic conductivity can be maintained over the long term remains an important and unsolved issue for both academia and industry [7].

The mechanisms of dynamic fracture permeability mainly include stress sensitivity, matrix shrinkage/swelling and gas slippage [8]. Regarding stress sensitivity, McKee et al. were the first to recognize that coal permeability varies exponentially with effective stress [9]. Palmer and Mansoori proposed a classical model accounting for the dual influence of stress and pore pressure [10]. Shi and Durucan incorporated cleat and matrix deformation into a unified stress-pore-pressure function based on a dual-porosity model and uniaxial-strain conditions [11,12]. Cui and Bustin pointed out that the volumetric strain induced by methane desorption strongly affects CBM productivity [13]. Regarding matrix shrinkage/swelling, Pan and Connell developed a theoretical model for gas-adsorption-induced coal swelling [14]. Chen et al. further introduced anisotropy and showed that the permeability parallel to bedding is more sensitive to stress [15]. Adsorption experiments show that matrix shrinkage/swelling is closely related to coal rank, pore structure, gas type and adsorption conditions [16–18]. Regarding multi-mechanism coupling, dual-porosity/dual-permeability and fully coupled diffusion-adsorption-deformation models have been developed [19–21]. Pulse-decay and displacement experiments show that the permeability to non-sorbing gases is controlled only by effective stress, whereas that to

CH_4 and CO_2 is strongly affected by matrix shrinkage/swelling [22,23]. For deep coal seams, triaxial experiments show that the permeability decreases by nearly two orders of magnitude when the confining pressure increases from 5 to 20 MPa [7], and fracture permeability is strongly influenced by in situ stress conditions, coal mechanical properties and effective stress [24,25]. Overall, existing studies have focused mainly on shallow coal seams and on coal permeability under effective stress, whereas the dynamic permeability response of the cleat-hydraulic fracture system in deep coal under high stress has received insufficient attention.

The interaction of water and its solutes with the coal matrix is another important aspect affecting fracture seepage capacity. According to the depth of the research focus, the relevant studies can be divided into three aspects: water saturation effects, salinity effects, and mineral dissolution/precipitation effects. Regarding water saturation, experiments show that the gas permeability of coal decreases with increasing water saturation and follows a power-law relation with net pressure [26]. Experiments under different water-bearing conditions show that permeability decreases exponentially with increasing water content and pore pressure, and that water affects both gas adsorption and adsorption-induced deformation [27]. Regarding salinity, experiments show that permeability decays negatively exponentially with effective stress and is positively correlated with salinity within a certain range. When salinity increases from 0 to 5000 ppm, the stress sensitivity decreases markedly, and it tends to stabilize as salinity rises further to 10,000 ppm [28]. The main mechanism is that, at low salinity, thickening of the hydration film, dispersion and migration of kaolinite particles, and interlayer hydration swelling of montmorillonite jointly damage the seepage channels. Regarding the effects of fracturing fluid and mineral dissolution-precipitation, studies show that an increase in ion concentration enhances the hydrophobicity of the coal surface, and that the action of fracturing fluid causes mineral dissolution and precipitation [29], producing changes in porosity and permeability and thereby significantly affecting the evolution of wetting-phase saturation and the gas production rate [30,31]. Most hydrochemistry-related studies focus on the effects of water saturation or salinity in shallow coal seams and generally indicate that hydrochemical treatment is largely detrimental to CBM seepage. However, for deep coal in which carbonate-filled cleats are widely developed, studies on the dynamic seepage response of cleat-hydraulic fractures under hydrochemical-stress coupling are still very limited, and the dynamic permeability evolution of fractures remains unclear. Specifically, it remains unclear (i) how the connectivity of cleats and hydraulic fractures controls the permeability level and stress sensitivity of deep coal under high effective stress, (ii) whether and to what extent hydrochemical treatment can modify the permeability of cleats and hydraulic fractures, and (iii) how the permeability characterization parameters should be determined and selected under different loading and unloading paths.

The mathematical characterization of the dynamic permeability of the fracture system is particularly important for productivity evaluation and development optimization. Permeability models are currently divided into stress-type and strain-type models, which take effective stress and adsorption strain as the control variables, respectively, and can be converted into each other through the elastic relations of porous media [32]. Stress-type models start from the exponential relation among permeability, porosity and effective stress [9–12,33], while strain-type models start mainly from the characterization of adsorption–swelling/shrinkage effects [13,14,34–36]. Many quantitative characterization models of different forms have been developed, but most are based on an exponential relation between the permeability ratio and the effective stress, or a power-law relation between permeability and strain. However, permeability characterization models are established mainly on the basis of effective stress or strain and do not directly consider fracture

structure or hydrochemical treatment, resulting in considerable uncertainty in the model parameters under different reservoir conditions [15,24]. In contrast to the above decoupled treatments, fully coupled flow-geomechanical studies emphasize the interaction between stress evolution, deformation and flow during reservoir pressure changes, for example, the coupled effects of pore pressure evolution, time-dependent deformation, and irreversible mechanical responses during pore pressure changes in natural gas hydrate-bearing sediments [37]. However, this study follows a different, deliberately simplified route which describes the permeability-effective stress relation by an exponential law, in which stress evolution is represented by the current effective stress and the irreversible, path-dependent deformation is not explicitly formulated but is instead captured implicitly by separately calibrated parameters for different loading and unloading paths. This simplification sacrifices a rigorous constitutive description of time-dependent deformation, but it enables rapid, experiment-based parameterization of the cleat-hydraulic fracture system, which is the main demand of fracturing and production-schedule design in this work. Therefore, for the dynamic permeability characterization of deep coal reservoirs, the fracture structure, effective stress and hydrochemical conditions of the reservoir must be reproduced so as to obtain the corresponding characterization parameters, which can then support the design of fracturing and production schedules.

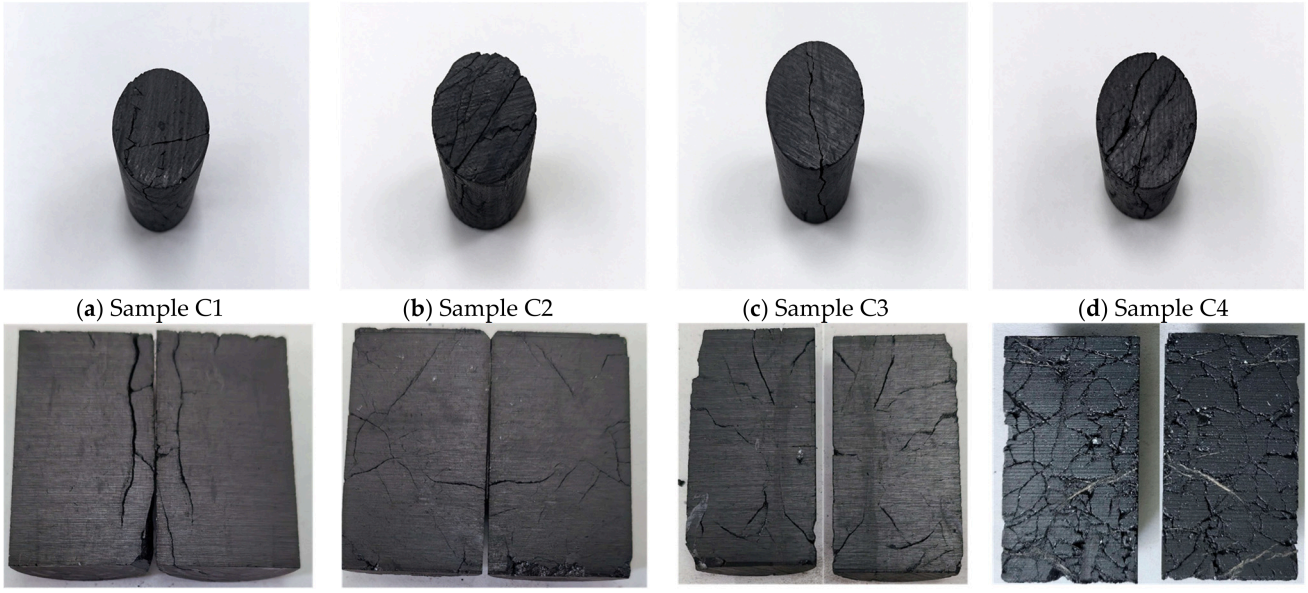
To address these issues, this study took the No. 8 deep coal of the Benxi Formation in the Ordos Basin as the research object and investigated the dynamic permeability evolution and characterization of the cleat-hydraulic fracture system under stress-hydrochemical coupling. First, overburden gas permeability experiments were carried out to characterize the dynamic permeability behavior of cleats with different degrees of connectivity and of pre-fractured (self-propped) hydraulic fracture samples under high effective stress. Second, the stress loading path was varied and hydrochemical treatment was applied to reveal the permeability evolution, the recoverability of fracture closure and the modification by calcite dissolution under stress-hydrochemical coupling. Finally, a model incorporating a cleat compression term and a slippage term was used for quantitative characterization to determine the distribution ranges of the fracture parameters under deep coal reservoir conditions and to achieve a deterministic characterization of the model parameters. The results provide basic parameters for the controlled-pressure production schedule design, hydraulic fracturing design and productivity evaluation of deep CBM wells, and are of significant engineering value.

2. Experiment Description

2.1. Coal Samples

The No. 8 coal of the Benxi Formation in the Ordos Basin is generally 2–15 m thick, up to 25 m at maximum, and is buried at a depth of 2000–4000 m in the central part of the basin. The present geothermal gradient of the reservoir is about 2.8 °C/100 m, the temperature ranges from 65 to 135 °C, and the reservoir pressure is 22–33 MPa. The average porosity is 5.42% and the average permeability is 2.32×10^{-3} μm^2. The pore structure is dominated by micropores (pore diameter < 2 nm, accounting for 42–57% by volume) and macropores (pore diameter > 50 nm, 28–45%), while mesopores (2–50 nm) account for only 13–15% [4]. The No. 8 coal is a dual-porosity medium containing both matrix pores and fractures, with a highly developed cleat system. Thin-section and microscopic cleat statistics show that cleats with an aperture larger than 5 μm have a relatively low density of 10–21 per 9 cm^2, whereas those with an aperture smaller than 5 μm are much denser, reaching 94–323 per 9 cm^2. Some fractures are filled, mainly with carbonate minerals such as calcite and with clay minerals [4].

The samples used in this study were taken from the No. 8 coal of the Benxi Formation in the Ordos Basin, at vertical depths of 2059–2425 m. Standard cylindrical plugs of Φ25 mm × 50 mm were drilled from the coal cores along the core axis and divided into two types according to fracture assemblage (Figure 1). The first type comprises intact samples, i.e., complete cylindrical coal plugs of Φ25 mm × 50 mm, numbered C1–C4 (four plugs), which were used to characterize the seepage and mechanical response of the cleat system under stress. Primary cleats are developed in all these coal samples, and the cleats in C3 and C4 run through the sample axially but the samples are not split. The second type comprises pre-fractured samples, prepared by splitting a Φ25 mm × 50 mm plug axially along its center into two halves and then rejoining them, numbered J1, J2-1, J2-2 and M1 (four plugs). The split surfaces simulate self-propped hydraulic fracture surfaces and, together with the inherent cleats of the coal, constitute a cleat-hydraulic fracture system. Among them, J1, J2-1 and J2-2 have comparable cleat development, and J1 contains an axially through-going cleat. M1 has particularly well-developed cleats, many of which are filled with calcite, and the cleats bubble conspicuously when titrated with hydrochloric acid.



(**a**) Sample C1 (**b**) Sample C2 (**c**) Sample C3 (**d**) Sample C4

(**e**) Sample J1 (**f**) Sample J2-1 (**g**) Sample J2-2 (**h**) Sample M1

Figure 1. Coal samples from the No. 8 coal of the Benxi Formation in the Ordos Basin: (**a**–**d**) intact samples C1–C4; (**e**–**h**) pre-fractured samples J1, J2-1, J2-2 and M1.

2.2. Experimental Setup

Overburden permeability testing of the coal samples was carried out on a Coreval 700 overburden gas porosimeter and permeameter manufactured by Vinci Technologies (Nanterre, HDS, France), as shown in Figure 2. The instrument can measure the permeability of standard cylindrical core samples of Φ25 mm × 50 mm under an overburden (confining) pressure of 2.76–68.95 MPa using helium as the medium (to avoid adsorption-induced swelling/shrinkage of the coal matrix). Its permeability measurement range is 0.001×10^{-3} μm^2 to 10 μm^2, and the maximum pore pressure is 1.72 MPa. The instrument mainly consists of a core holder, pressure transducers, gas-line control valves, and a data acquisition and computation workstation. During measurement, the sample is loaded into the holder and the set confining pressure is applied, after which the permeability is determined by the unsteady-state pressure decay method. By presetting a series of confining pressures, the instrument automatically completes permeability tests at different confining pressures in sequence.

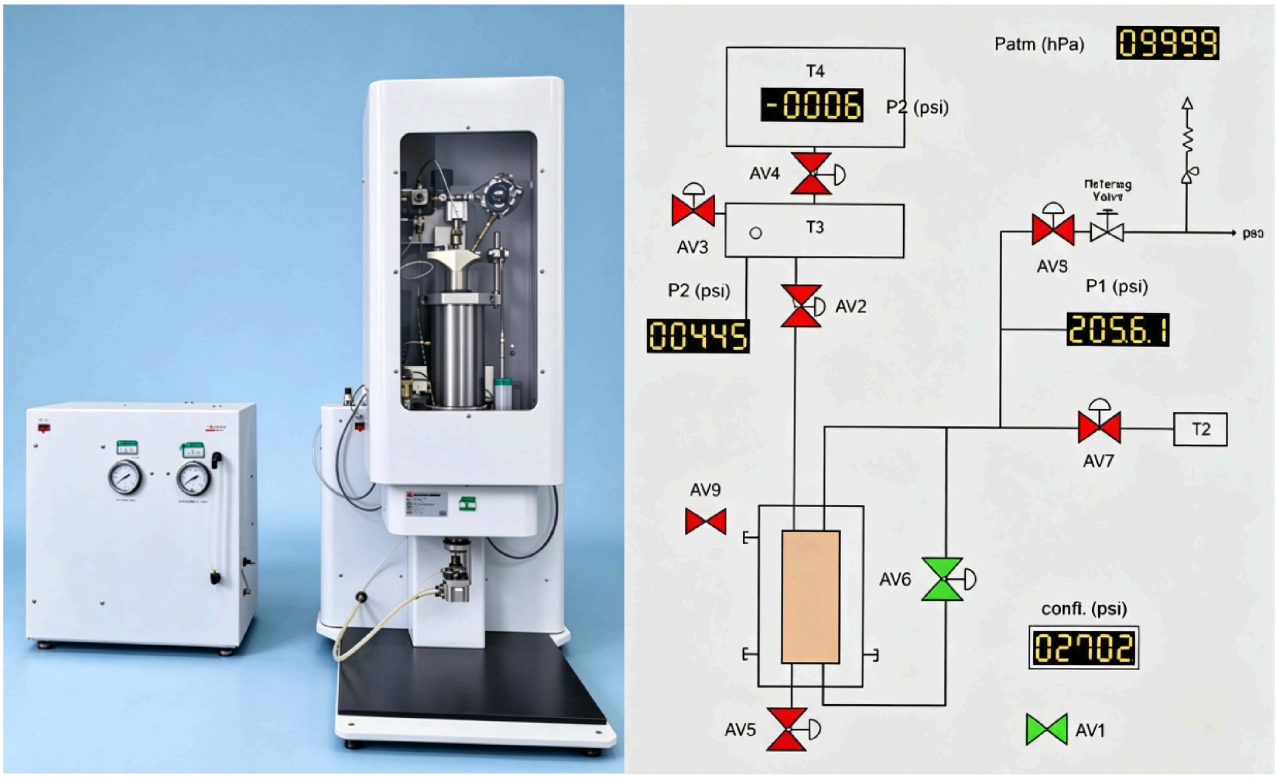


Figure 2. Schematic of the experimental setup.

2.3. Experimental Condition

This experiment aims to investigate the dynamic permeability characteristics of coal samples and to provide data support for analyzing the evolution of dynamic permeability under different fracture types, loading modes (including stepwise loading, unloading and secondary loading) and hydrochemical treatment. To this end, two types of coal samples were studied to characterize the seepage response under different fracture-system characteristics: intact samples (C1–C4) and pre-fractured samples (J1, J2-1, J2-2 and M1). The test fluid (pore) pressure was set to 1.38 MPa, and the confining pressure was applied in a stepwise manner, set successively to 3.45, 6.90, 12.41, 17.24 and 24.14 MPa. The loading mode and test numbering of each sample are listed in Table 1. (1) The intact samples C1–C4 were all tested under stepwise loading in the dry state. (2) The pre-fractured sample J1 was first tested under stepwise loading in the dry state (J1), then subjected to a secondary loading test on the same sample (J1-S), and finally measured under stepwise unloading (stress recovery) after the J1-S test (J1-S-R). (3) J2-1 and M1 were first tested under stepwise loading in the dry state, then subjected to a secondary loading test after hydrochemical treatment (J2-1w and M1w), and finally tested under stepwise unloading (J2-1w-R and M1w-R). (4) J2-2 was tested under stepwise loading in the dry state (J2-2) and then under stepwise unloading (J2-2-R). Through the above stress-path design of loading-secondary loading-hydrochemical treatment-unloading, permeability evolution data were obtained for the cleats, the hydraulic fractures and their combined system under coupling of different fracture characteristics, loading modes and hydrochemical environments. The hydrochemical treatment was performed by soaking the samples in water in an open beaker at ambient temperature and pressure for 24 h. The soaked samples were then taken out and air-dried in air for 12 h before the overburden permeability test.

Table 1. Coal samples and the respective experimental conditions.

Sample Type	Sample No.	Vertical Depth, m	Test ID	Test Condition
Intact sample	C1	2306.73	C1	Dry sample under stepwise loading stage
	C2	2300.50	C2	
	C3	2302.44	C3	
	C4	2301.11	C4	
Pre-fractured	J1	2425.20	J1	Dry sample under stepwise loading stage
			J1-S	Secondary loading stage after J1
			J1-S-R	Stepwise unloading stage after the J1-S test
	J2-1	2424.80	J2-1	Dry sample under stepwise loading stage
			J2-1w	Secondary loading stage of J2-1 after hydrochemical treatment
			J2-1w-R	Stepwise unloading stage after the J2-1w test
	J2-2	2424.85	J2-2	Dry sample under stepwise loading stage
			J2-2-R	Stepwise unloading stage after the J2-2 test
	M1	2059.81	M1	Dry sample under stepwise loading stage
			M1w	Secondary loading stage of M1 after hydrochemical treatment
			M1w-R	Stepwise unloading stage after the M1w test

3. Results and Discussion

3.1. Results for Samples with Different Fracture Types

Figures 3 and 4 show the variation in permeability with confining pressure for coal samples with different fracture types. Overall, as the confining pressure increases stepwise from 3.45 to 24.14 MPa, the permeability of all samples shows a marked exponential decline, indicating that stress closure strongly controls the permeability of cleats and fractures. For the intact samples, the development and connectivity of cleats dominate their permeability level: C1 and C2, whose cleats are not directly connected, have initial permeabilities of only 0.204×10^{-3} μm^2 and 0.848×10^{-3} μm^2 at 3.45 MPa, whereas C3 and C4, which each contain a directly through-going cleat, reach 2.45×10^{-3} μm^2 and 4.62×10^{-3} μm^2, respectively, i.e., a single directly through-going cleat can increase the initial permeability of an intact sample by about 5–10 times. At the same time, the stress sensitivity of the samples with a directly through-going cleat is markedly lower: when the confining pressure increases to 24.14 MPa, the permeability of C1 and C2 decays by about 490 and 1400 times, respectively, whereas that of C3 and C4 decays by only about 215 and 104 times, indicating that a directly through-going cleat can still maintain good seepage capacity at relatively high effective stress. For the pre-fractured (self-propped) samples, under comparable cleat development, their permeabilities are comparable to those of intact samples containing a directly through-going cleat: the initial permeabilities of J1, J2-2 and J2-1 are 3.90×10^{-3} μm^2, 3.32×10^{-3} μm^2 and 1.17×10^{-3} μm^2, respectively, which are of the same order as those of C3 (2.45×10^{-3} μm^2) and C4 (4.62×10^{-3} μm^2). When the cleats are very well developed and well connected (M1), the sample permeability increases markedly: the initial permeability of M1 is as high as 32.36×10^{-3} μm^2, about 8–30 times higher than that of the other pre-fractured samples, and it remains 2.40×10^{-3} μm^2 when the confining pressure increases to 24.14 MPa, with an overall decay of only about 13 times, showing the strongest seepage

capacity and the weakest stress sensitivity. The above results indicate that the connectivity of cleats and the presence and connectivity of hydraulic fractures jointly determine the seepage capacity of coal. In addition to the high-conductivity fractures created by hydraulic fracturing, well-connected cleats are the key to maintaining high-productivity seepage channels in deep coal reservoirs.

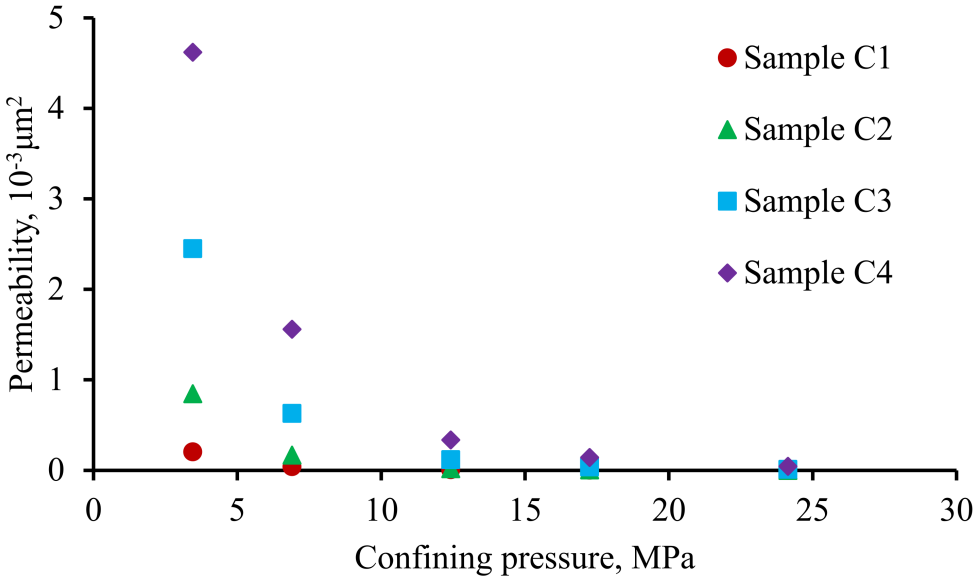


Figure 3. Results for intact coal samples C1~C4 under stepwise loading stage.

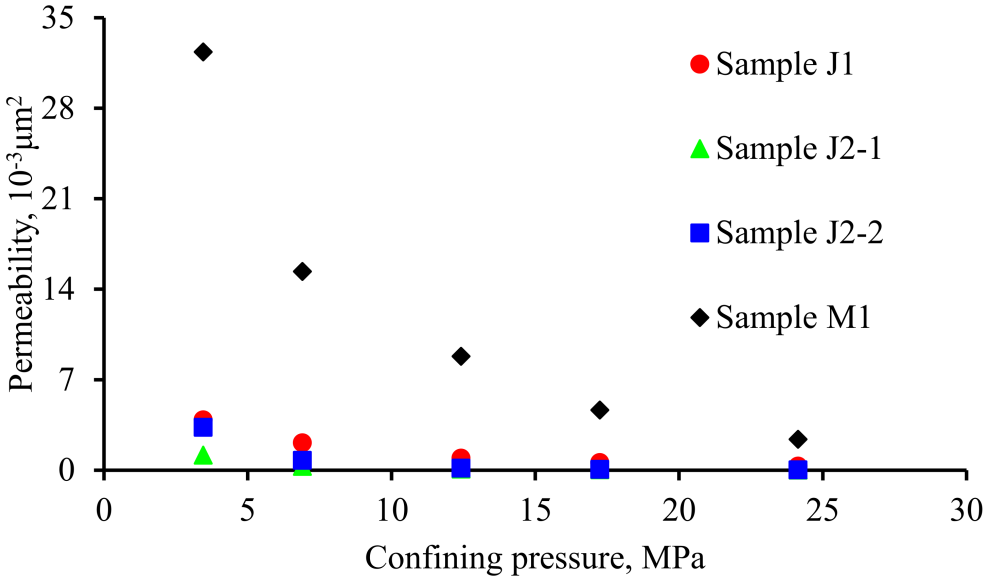


Figure 4. Results for pre-fractured coal samples under stepwise loading stage.

3.2. The Effects of Hydrochemical Treatment

To further examine the effect of hydrochemical treatment on the permeability of cleats and hydraulic fractures, secondary loading tests were carried out on J2-1 and M1 after soaking–air drying and compared with the results of J1-S, which underwent secondary loading directly without hydrochemical treatment (Figures 5–7). The results show that the influence of hydrochemical treatment on permeability is closely related to the characteristics of the fracture system of the coal sample. For J2-1, with moderately developed cleats, the permeability at each confining pressure after soaking–air drying is generally 30–65% higher

than that of the first loading (e.g., from 1.17 × 10^{-3} μm^2 to 1.52 × 10^{-3} μm^2 at 3.45 MPa, and from 0.020 × 10^{-3} μm^2 to 0.033 × 10^{-3} μm^2 at 24.14 MPa, reaching about 1.3–1.65 times). Compared with J1-S, which did not undergo hydrochemical treatment, secondary loading reduces the sample permeability by 20–40%, indicating that the seepage improvement produced by hydrochemical treatment is sufficient to offset and exceed the compaction damage caused by secondary loading. For M1, with well-developed cleats originally filled with calcite, the increase in permeability after soaking–air drying is particularly pronounced: at each confining pressure it reaches 2.0–3.7 times the value at the same confining pressure before treatment, and the overall permeability decay factor from 3.45 to 24.14 MPa decreases from about 13 to about 7.5 times, indicating a marked reduction in stress sensitivity. It is considered that, because M1 has well-developed cleats filled with calcite, carbonate cements such as calcite are dissolved during soaking, interconnecting the originally cemented and sealed cleats and natural fracture network and creating new flow channels, so that its hydrochemical gain is much higher than that of J2-1 with moderately developed cleats. In summary, hydrochemical treatment is a factor that cannot be neglected in the evolution of the seepage capacity of coal reservoirs, and its influence is controlled by the degree of cleat development and the mineral filling characteristics.

During hydrochemical treatment, calcite dissolves mainly along two reaction paths: (1) Hydrolysis, $CaCO_3 + H_2O \rightleftharpoons Ca^{2+} + HCO_3^- + OH^-$, which is slow and tends to equilibrium as OH^- accumulates and the solution pH rises, showing a self-inhibiting character. (2) Proton-promoted dissolution, in which dissolved CO_2 forms carbonic acid and releases H^+ ($CO_2 + H_2O \rightleftharpoons H_2CO_3 \rightleftharpoons H^+ + HCO_3^-$), and H^+ attacks the CO_3^{2-} on the calcite surface ($CaCO_3 + H^+ \rightarrow Ca^{2+} + HCO_3^-$). This rate is markedly higher than that of the hydrolysis path and is the dominant mechanism under open soaking conditions. In an open system, atmospheric CO_2 continuously dissolves into the solution, replenishing H^+ and neutralizing the OH^- produced by hydrolysis, thereby suppressing the rise in pH and allowing dissolution to proceed continuously. After the filling calcite is dissolved, the originally cemented and sealed cleats and natural fractures reopen and interconnect, forming more continuous seepage channels, which macroscopically manifests as an increase in permeability and a decrease in stress sensitivity.

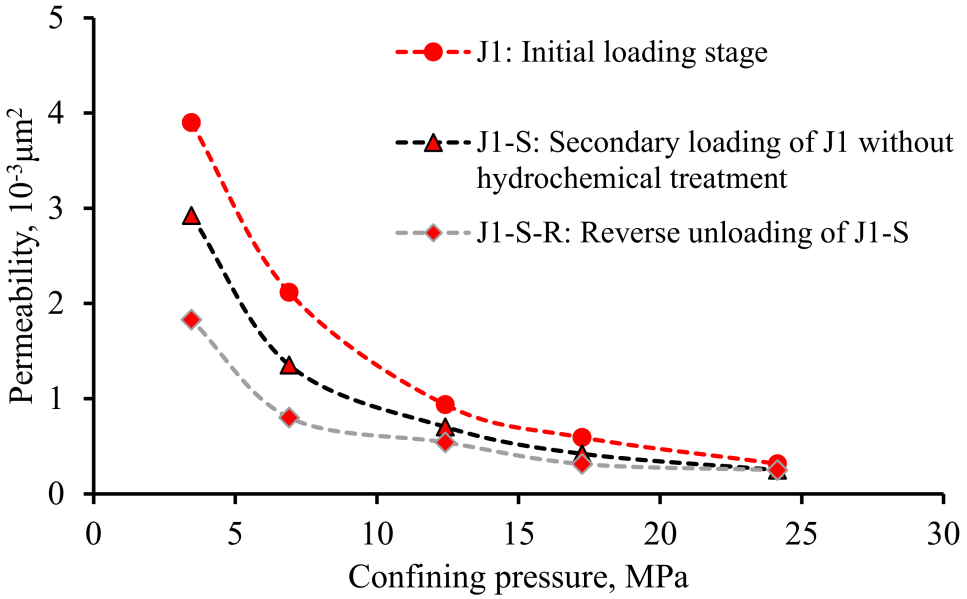


Figure 5. Results for J1 under stepwise loading (J1), secondary loading (J1-S), and successive unloading (J1-S-R).

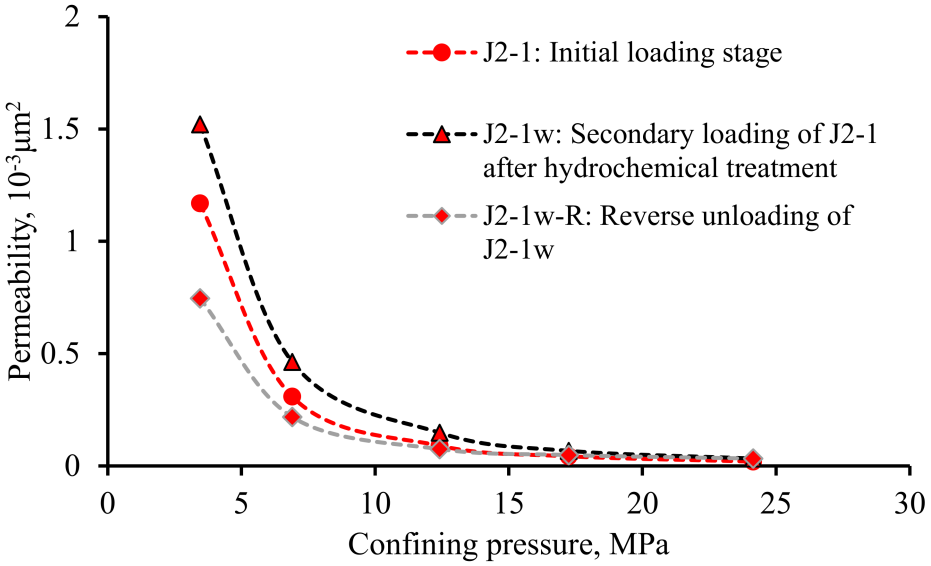


Figure 6. Results for J2-1 under stepwise loading (J2-1), secondary loading after hydrochemical treatment (J2-1w), and successive unloading (J2-1w-R).

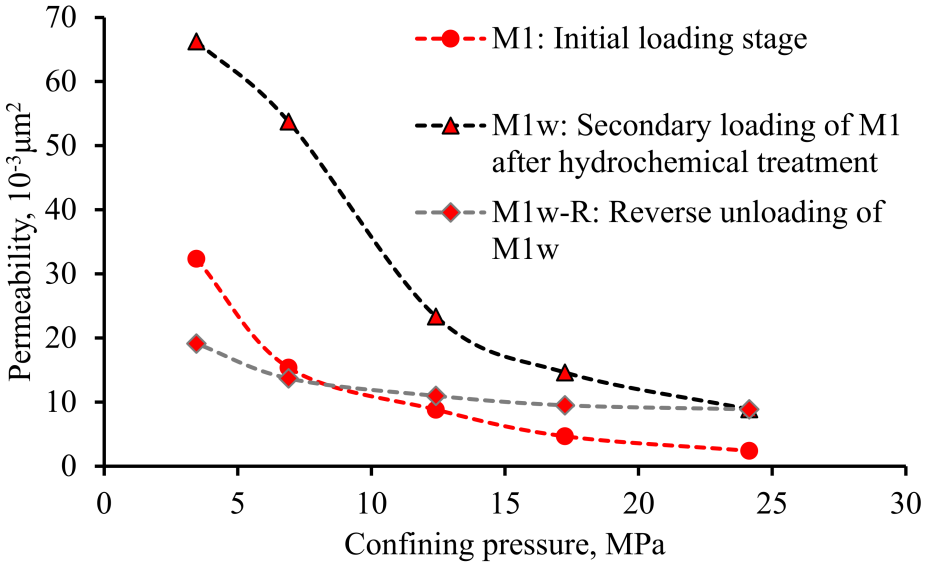


Figure 7. Results for M1 under stepwise loading (M1), secondary loading after hydrochemical treatment (M1w), and successive unloading (M1w-R).

It should be emphasized that the above interpretation has limitations. The hydrochemical treatment consisted only of soaking the samples in water in an open beaker for 24 h followed by air-drying for 12 h. The pH is about 6.0, but the dissolved-ion concentrations and dissolved mineral mass were not measured, so the contribution of calcite dissolution cannot be directly quantified from water-chemistry data. The inference relies mainly on the mineralogical evidence that the cleats of M1 are filled with calcite (confirmed by hydrochloric acid titration) and on the observed permeability and stress-sensitivity changes. Moreover, because the samples were soaked and subsequently dried, other processes may also have contributed to the permeability changes, including changes in the fracture-surface contact conditions caused by softening of clay minerals at fracture surfaces, migration and re-deposition of coal fines generated during soaking, and microcracking or shrinkage effects induced by drying. Therefore, the permeability enhancement after soaking–air drying should be regarded as the combined result of the above processes rather

than being attributed solely to calcite dissolution, although calcite dissolution can be the most probable attribute. Direct chemical analysis of the soaking solution before and after treatment, mineralogical characterization (e.g., XRD or CT scanning) of the samples, and dedicated tests isolating individual mechanisms are needed to verify and quantify the proposed interpretation, and this is left for future work.

3.3. The Effects of Confining Pressure Loading Scheme

The loading path (first loading, secondary loading and unloading) has a marked effect on coal permeability (Figures 5–7). At the same confining pressure, the permeability of J1 under secondary loading (J1-S) without hydrochemical treatment is generally about 20–40% lower than that under first loading, indicating that partial irreversible closure of the cleats and hydraulic fractures occurred during the first loading. In the unloading (stress recovery) stage, the permeability rebounds as the confining pressure decreases stepwise, but at the same confining pressure it recovers to only 35–60% of the first-loading level (mostly about 50%). For example, when J1-S-R is unloaded to 3.45 MPa, the permeability is 1.83×10^{-3} μm^2, only 47% of the first-loading value of J1, 3.90×10^{-3} μm^2. The loading and unloading curves do not coincide and show pronounced hysteresis, indicating that the closure of the fracture system is dominated by plastic deformation with limited elastic recovery, and that the permeability loss cannot be fully recovered. It is worth noting that the hydrochemically treated samples still retain part of the gain after stress cycling. The permeability of J2-1w-R at relatively high confining pressures (≥17.24 MPa) is even higher than the corresponding value of J2-1 under first loading. In addition, the unloading permeability of M1w-R in the range of 12.41–24.14 MPa ($8.86–10.98 \times 10^{-3}$ μm^2) is also higher than the corresponding value of M1 under first loading ($2.40–8.81 \times 10^{-3}$ μm^2), indicating that the flow channels created by hydrochemical treatment have a certain resistance to stress closure. At the same time, however, when M1w-R is unloaded to a low confining pressure (3.45 MPa, 19.14×10^{-3} μm^2), the permeability is still markedly lower than the corresponding value of its loading curve (66.28×10^{-3} μm^2), indicating that repeated loading–unloading still causes significant permeability loss. The above results show that the stress path strongly affects the evaluation of coal permeability. For CBM production, most of the fracture-permeability loss caused by repeated fluctuations in bottom-hole pressure is irreversible, so a reasonable production schedule (stress path) is of great significance for maintaining the permeability of coal reservoirs.

3.4. Characterization of the Dynamic Permeability of Cleat-Hydraulic Fractures

3.4.1. Theoretical Model for the Characterization of the Dynamic Permeability

Many models are currently available for the quantitative characterization of the permeability of coal fracture systems, and their mechanistic explanations mainly involve three aspects: the cleat compression and stress sensitivity caused by increasing effective stress, the matrix shrinkage effect caused by gas adsorption–desorption, and the gas slippage effect under low pressure. A large number of characterization models have been proposed in these aspects [9–14,32–35]. In this study, based on the model proposed by Shi and Durucan [11,12], the relationship between permeability and effective stress was fitted and the parameters were inverted, so as to further characterize the influence of cleat type, loading scheme and hydrochemical treatment on the model parameters and to provide basic parameters for the quantitative characterization of deep coal permeability.

Effective stress controls permeability mainly by affecting the degree of opening of the pore and fracture structures of coal, thereby governing permeability. When the slippage

and adsorption–swelling effects are neglected, the widely used permeability-effective stress relationship takes an exponential form:

$$k = k_0 e^{-3c_f(\sigma-\sigma_0)} \quad (1)$$

where σ and σ_0 are the effective stresses acting on the fracture system under the current and initial conditions, respectively, in MPa; c_f is the cleat (fracture) volume compressibility, i.e., the permeability coefficient, in MPa^{-1}; k and k_0 are the permeabilities under the current and initial conditions, respectively, in 10^{-3} μm^2.

When the adsorption–swelling effect is neglected, the effective stress can be simplified as the difference between the in situ stress (the applied confining pressure in the experiments) and the pore pressure:

$$\sigma = \sigma' - \alpha p \quad (2)$$

where σ' is the in situ stress (the applied confining pressure in the experiments), MPa; p is the reservoir pore pressure, MPa; α is the Biot coefficient, taken as 1 in this study.

Based on the Shi-Durucan model, the matrix shrinkage effect caused by adsorption–desorption is also characterized by a corrected effective stress, which can be expressed as:

$$\sigma - \sigma_0 = (\sigma' - \alpha p) - (\sigma_0{}' - \alpha p_0) + \frac{E\varepsilon_L}{3(1-v)}\left(\frac{p}{p+p_L} - \frac{p_0}{p_0+p_L}\right) \quad (3)$$

where $\sigma_0{}'$ is the initial in situ stress, MPa; E is the elastic modulus of coal, MPa; v is Poisson's ratio; ε_L is the ultimate adsorption strain; and PL is the Langmuir pressure, MPa.

At low pore pressure, the permeability change caused by the gas slippage effect must also be considered, and the permeability expression is modified as follows:

$$k = k_0\left(1 + \frac{b}{\overline{p}}\right)e^{-3c_f(\sigma-\sigma_0)} \quad (4)$$

where b is the Klinkenberg slippage factor, MPa; $\overline{p}$ is the mean pore pressure, MPa.

In the present experiments, the pore pressure was constant at 1.38 MPa and the flowing medium was helium (He). Because helium molecules are small and are hardly adsorbed by the coal matrix, the matrix shrinkage effect caused by adsorption can be neglected. Moreover, because the pore pressure was identical at all test levels, the influence of the slippage effect on permeability remained constant within the experimental stress range and can be incorporated into the initial permeability term. The permeability expression is thus simplified to:

$$\ln k = \ln k_0 - 3c_f(\sigma - \sigma_0) \quad (5)$$

Based on the above equation, the experimental results in Sections 3.1–3.3 were linearly fitted with $\ln k$ as the ordinate and $(\sigma - \sigma_0)$ as the abscissa. The fitted slope corresponds to $-3c_f$, and the intercept corresponds to $\ln k_0$. These can quantitatively characterize the stress sensitivity of the sample and the permeability level at the reference effective stress. In the analysis, the effective stress under the original reservoir pore pressure and the minimum horizontal principal stress is taken as σ_0. The minimum horizontal principal stress is 38.3 MPa and the original reservoir pore pressure is 21 MPa, giving a σ_0 of 17.3 MPa.

As can be seen from Figures 8–12, the $\ln k$ and $(\sigma - \sigma_0)$ of the samples are not strictly linear over the whole range: when $(\sigma - \sigma_0) > -10$ MPa, the data points show a good linear relationship with small regression residuals, whereas when the effective stress is significantly lower than the in situ condition (in this study, $(\sigma - \sigma_0) < -10$ MPa) the data points begin to deviate markedly from the regression line. The reasons are as follows. First, the cleat volume compressibility c_f is not constant: at low effective stress the cleats are

open and the fracture surfaces have few contact points, so a unit stress increment causes a larger change in aperture and permeability. As the effective stress increases, the cleats are progressively compacted and the contact area of the fracture surfaces increases, so the compressibility decreases accordingly and the $\ln k$ and $(\sigma - \sigma_0)$ relationship approaches a straight line only then. Second, after the cores are recovered from the formation they experience stress release, and some microfractures that were closed under in situ conditions reopen at low effective stress, so the composition of the seepage channels in the lower effective stress range differs from the actual reservoir state, whereas the higher effective stress range is more applicable. Third, in the lower effective stress range the fracture apertures are large, the permeability and gas flow rate are high, and the relative influence of non-Darcy (inertial) effects increases, so that the lower the effective stress, the more obvious the deviation from the straight line. Therefore, the data in the higher effective stress range ($(\sigma - \sigma_0) > -10$ MPa, close to the original formation effective stress) were used for fitting, so that the fitting results better represent the compression characteristics of the fracture system under in situ reservoir conditions.

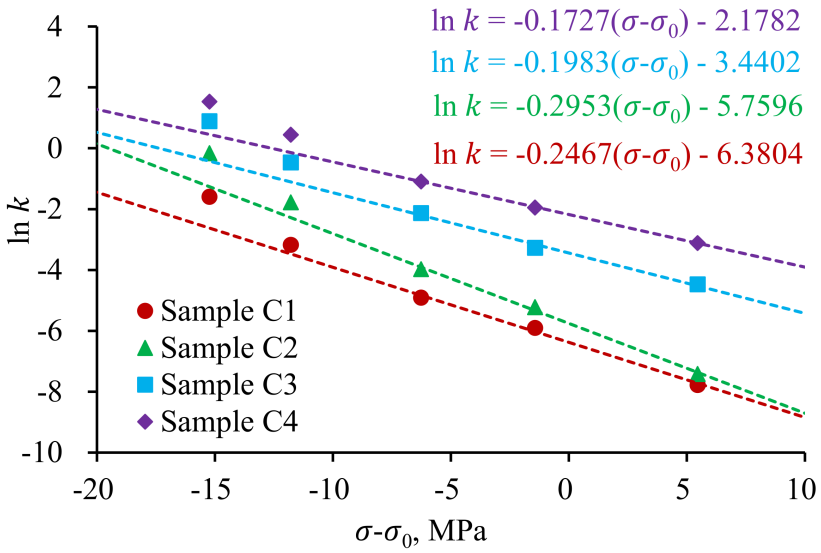


Figure 8. Permeability characterization results of intact coal samples C1~C4.

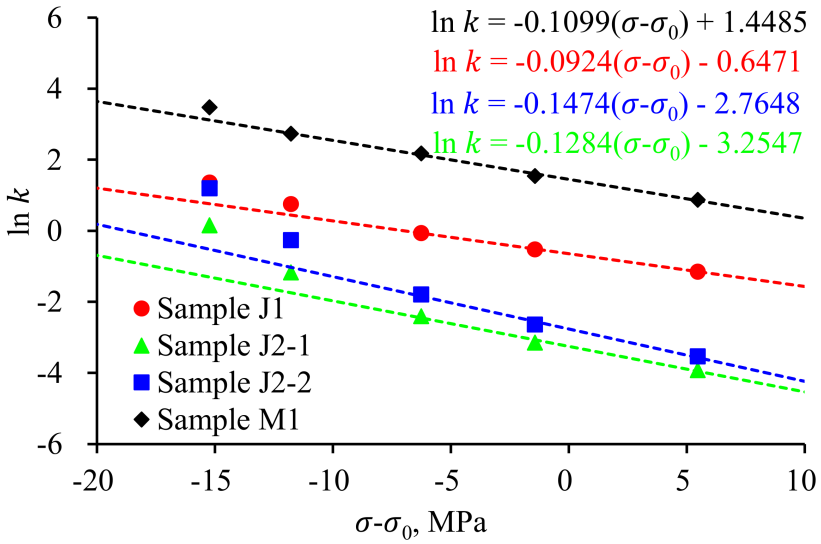


Figure 9. Permeability characterization results of pre-fractured coal samples.

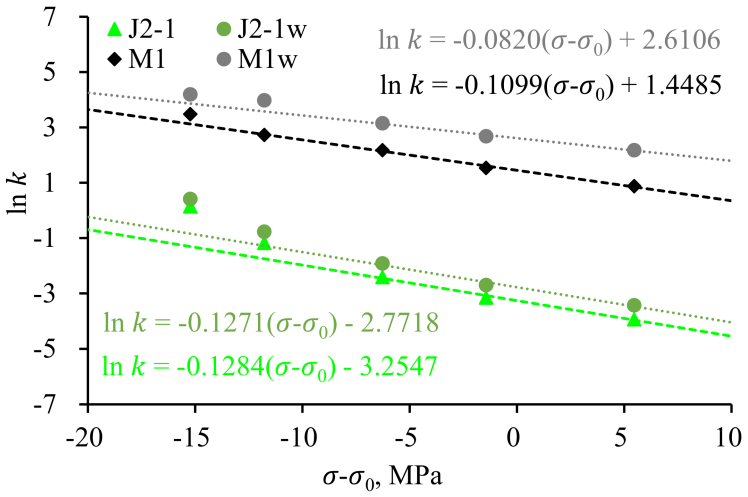


Figure 10. Comparison of permeability characterization results of samples before and after hydrochemical treatment.

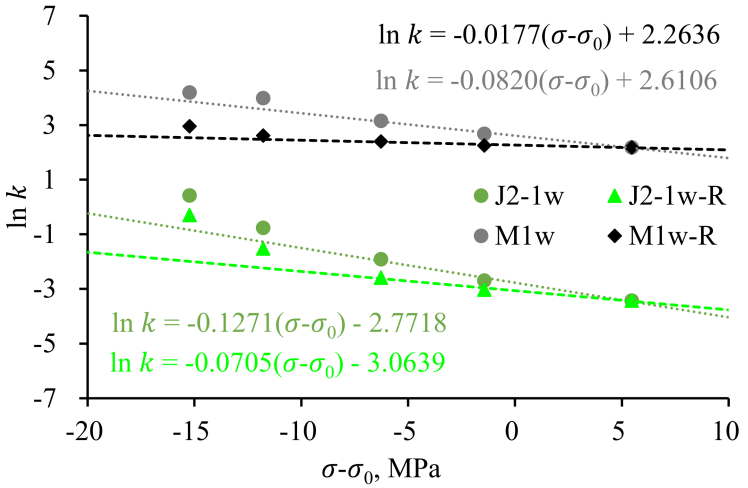


Figure 11. Comparison of permeability characterization results of samples under stepwise loading and unloading stages.

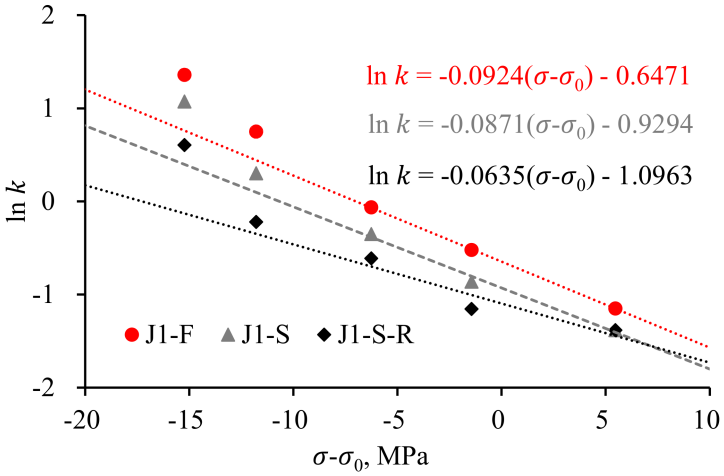


Figure 12. Comparison of permeability characterization results of sample J1 under stepwise loading, secondary loading and unloading stages.

In this study, laboratory results are extrapolated to reservoir conditions under the assumption that permeability is identical at equal effective stress. Effective stress is calculated

as confining pressure minus pore pressure for laboratory tests, and as minimum horizontal stress minus pore pressure under in situ reservoir conditions. Nevertheless, uncertainties remain when extrapolating the fitted exponential relationship to reservoir pressure (stress) conditions that differ from the experimental ones. First, the experiments covered an effective stress range of about 2.1–22.8 MPa, but other in situ conditions for other formations may be different. In addition, the fitted compressibility itself varies with the stress level over which the regression is performed, so different fitting windows yield slightly different parameter values. Therefore, the calibrated parameters should be regarded as experiment-based characterizations of the stress sensitivity of the cleat and cleat-hydraulic fracture systems rather than as universally applicable reservoir values. When used for field-scale permeability prediction under different reservoir pressures, they should be recalibrated or corrected for gas type, temperature, and stress level, and the prediction uncertainty should be evaluated.

3.4.2. Characterization of the Dynamical Permeability with Different Fracture Types

Figure 8 shows the variation in the $\ln k$ with $(\sigma - \sigma_0)$ and the linear fitting results for the intact samples (C1–C4). The permeability coefficients c_f of C1–C4 are 0.2467, 0.2953, 0.1983 and 0.1727 MPa^{-1}, respectively, and the original permeabilities are 0.0017, 0.0032, 0.0321 and 0.1133 $\times 10^{-3}$ μm^2, respectively. The c_f of C1 and C2, whose cleats are not directly connected, is markedly higher than that of C3 and C4 with directly through-going cleats, consistent with the pattern revealed in Section 3.1: non-through-going cleats tend to close directly under effective stress and the seepage has to bypass the coal matrix, so they respond more sensitively to stress increments. By contrast, through-going cleats provide continuous channels for seepage and have alternative paths through the adjacent fracture network, so that after part of a cleat closes the fluid can be redistributed, giving both a higher permeability baseline and lower stress sensitivity.

Figure 9 shows the fitting results of permeability versus effective stress difference for the pre-fractured samples (J1, J2-1, J2-2 and M1). The permeability coefficients c_f of the four pre-fractured samples range from 0.0924 to 0.1474 MPa^{-1}, generally lower than those of the intact samples (0.1727–0.2953 MPa^{-1}), indicating that the self-propped fracture surfaces are dominated by elastic contact deformation of the asperities during loading and have a higher compression stiffness than the coal matrix cleat system, so that the permeability decays relatively gently with effective stress. Among the four samples, the intercept of M1 is much higher than those of the others, reflecting that the well-developed cleat network provides the highest initial permeability. The permeability coefficient c_f of J1 is the smallest, followed by that of M1, indicating that the connectivity of the cleat-hydraulic fracture system determines the difference in stress sensitivity among the pre-fractured samples.

3.4.3. Characterization of the Dynamical Permeability with Hydrochemical Treatment

Figure 10 compares the fitted $\ln k$ versus $(\sigma - \sigma_0)$ relationships of samples J2-1 and M1 before and after soaking–air drying. For J2-1, with moderately developed cleats, the slope of the fitted line is almost unchanged before and after treatment, while the intercept rises from −3.2547 to −2.7718 (permeabilities of 0.0386 and 0.0625 × 10^{-3} μm^2, respectively), i.e., soaking–air drying increases the permeability at the same effective stress to about 1.6 times the pre-treatment value overall, while the stress-sensitivity coefficient remains essentially unchanged. This indicates that, for this sample, the hydrochemical treatment mainly dissolves and enlarges the existing seepage channels and connects them, without markedly changing the compression stiffness of the coal matrix and the cleat system.

For M1, with well-developed cleats filled with calcite, the intercept rises from 1.4485 to 2.6106 after treatment ($\Delta \ln k \approx 3.2$), at the same effective stress the permeability increases to about 3.2 times. One should note that the 3.2 times is the value at the initial effective-stress

condition of the formation and based on the fitted parameter), and the stress-sensitivity coefficient decreases from 0.037 to 0.027 MPa^{-1} (a reduction of about 25%), i.e., soaking–air drying substantially raises the seepage baseline while markedly reducing the stress sensitivity. The reason is that the natural fractures in M1 are filled with carbonate minerals such as calcite, and during soaking–air drying the filling is partially dissolved, so the originally cemented and sealed cleats and natural fractures reopen and interconnect, forming more continuous and closure-resistant seepage channels, which increases the permeability level while reducing the overall compressibility of the fracture network. A comparison of J2-1 and M1 shows that both the improvement in permeability and the modification of stress sensitivity by hydrochemical treatment are jointly controlled by the degree of cleat development and the mineral filling characteristics. Therefore, low-concentration acid fracturing or post-fracturing acid injection can dissolve the filling calcite within a relatively short time and connect the sealed natural fractures. Moreover, because the action time is short, it avoids coal softening and the production of large amounts of coal fines, and is expected to become an important potential measure for enhancing production and recovery of deep coalbed methane, as well as the focus of subsequent research in this paper.

3.4.4. Characterization of the Dynamical Permeability with Different Loading Schemes

Figure 11 shows the fitting results of the samples in the stepwise unloading (stress recovery) stage after hydrochemical treatment. The fitted slopes of J2-1w-R and M1w-R are clearly lower than those of their loading stages J2-1w and M1w, and their intercepts decrease. The unloading-stage $\ln k$ versus $(\sigma - \sigma_0)$ relationships lie overall below those of the loading stages and are flatter, indicating that during unloading the permeability recovers along a path of lower recovery rate and cannot return to the pre-loading level at the same effective stress. The hysteresis effect is pronounced, and the fracture-surface closure contains an irreversible plastic-deformation component. Figure 12 shows the fitting results for sample J1, which did not undergo hydrochemical treatment, under first loading (J1-F), secondary loading (J1-S), and stepwise unloading (J1-S-R): the slopes of J1-S and J1-F are essentially the same while the intercept decreases corresponding to a decrease in permeability at the same effective stress, indicating that the permeability loss caused by secondary loading originates mainly from irreversible deformation of the fracture-surface rock during the first loading, whereas the compression stiffness of the cleat system itself is unchanged. The slope of the unloading stage of J1-S-R decreases further and the permeability recovery is incomplete, showing the same hysteresis effect as J2-1w-R and M1w-R.

It should be noted that the exponential model in Section 3.4.1 takes the current effective stress as the only state variable, whereas the above results clearly show that permeability is also path-dependent. At the same effective stress, the permeability under secondary loading is 20–40% lower than that under first loading, and the permeability during unloading recovers to only 35–60% of the first-loading level. In other words, the irreversible (plastic) deformation accumulated during stress history is not explicitly formulated in the model but is implicitly embedded in the calibrated parameters, which therefore differ between stress paths. When the model is used to predict permeability under different loading and unloading paths, the parameters should be selected according to the stress path actually experienced: for first loading or increasing effective stress (e.g., reservoir pressure drawdown on a virgin reservoir), the compressibility and reference permeability fitted from the first-loading stage should be used; for repeated loading (e.g., fluctuating bottom-hole pressure), the secondary-loading parameters, which embody the irreversible loss, should be adopted; and for unloading or stress recovery (e.g., shut-in or pressure build-up stages), the unloading-stage parameters should be used, because they describe the lower recovery path. Using a single parameter set calibrated only from first loading would overestimate

the permeability during re-loading and unloading, so path-specific parameter sets, such as those determined in this study, are recommended for practical prediction.

In this study, the No. 8 deep coal of the Benxi Formation in the Ordos Basin was taken as the object, and the permeability evolution of the cleat-hydraulic fracture system under different fracture types, stress states and hydrochemical treatment was systematically investigated by overburden permeability experiments. The ranges of the permeability and of the quantitative characterization parameters (initial permeability k_0, cleat compressibility c_f) under different conditions were obtained, and the characterization of the uncertain parameters in the permeability model was achieved. Based on Equation (4), the permeability of coal reservoirs can be quantitatively predicted. The results provide basic data support for the development design and production-schedule optimization of deep CBM wells. Moreover, based on the experimental finding that hydrochemical dissolution of calcite-filled fractures can significantly enhance permeability and reduce stress sensitivity, the following potential stimulation research direction is proposed: low-concentration acid fracturing or post-fracturing acid injection to activate natural fracture networks.

4. Conclusions

In this study, the permeability evolution of the cleat-hydraulic fracture system in deep coal under different fracture types, stress loading paths and hydrochemical treatment was investigated, and the parameters of the permeability model were quantitatively characterized. The main conclusions are as follows:

(1) The seepage capacity of coal is mainly controlled by the type and connectivity of the fracture system. The permeability of all samples decays exponentially with increasing effective stress. The connectivity of cleats and their connection with hydraulic fractures determine the initial permeability level and the stress sensitivity: the better the connectivity, the higher the initial permeability and the weaker the stress sensitivity. In addition to the high-conductivity fractures created by hydraulic fracturing, throughgoing and well-connected cleats are the key to maintaining high-productivity seepage channels in deep coal reservoirs.

(2) The stress loading path significantly affects permeability, and fracture closure is markedly irreversible. Repeated loading reduces the permeability at the same effective stress step by step. During unloading (stress recovery) the permeability rebounds, but the loading and unloading curves do not coincide and show pronounced hysteresis, indicating that fracture closure involves plastic deformation with limited elastic recovery. For CBM wells, most of the conductivity loss caused by repeated fluctuations in bottom-hole pressure is irreversible, so adopting a reasonable pressure-drawdown production schedule is important for maintaining reservoir permeability.

(3) Hydrochemical treatment can improve the conductivity of fractures to a certain extent, and the effect mainly depends on the degree of fracture development and the characteristics of the filling minerals. Dissolution of the filling carbonate minerals during soaking interconnects the originally cemented and sealed cleats, thereby enhancing permeability while reducing stress sensitivity. For samples with poorly developed or sparsely filled fractures, the improvement is limited. This suggests that fracture conductivity can be optimized by regulating the intensity and duration of the hydrochemical treatment, and that low-concentration acid fracturing or post-fracturing acid injection to activate filled natural fracture networks is a potential stimulation direction.

(4) The exponential model of dynamic fracture permeability versus effective stress describes the experimental results well, and the distribution of the stress-sensitivity coefficient of the cleat-hydraulic fracture system in the study area was obtained: 0.1727–0.2953 MPa^{-1} for the cleat system and 0.0924 to 0.1474 MPa^{-1} for the cleat-

hydraulic fracture system. After hydrochemical treatment, the permeability of the samples at the same effective stress increases to 1.3–1.65 and 2.0–3.7 times, respectively, for samples with moderately (like J2-1) and well-developed cleats (like M1), while the stress-sensitivity coefficient decreases to some extent. These results achieve a quantitative characterization of the uncertain parameters in the permeability model and provide a parameter basis for predicting fracture permeability in deep coal reservoirs.

Author Contributions: Conceptualization, D.L. and Y.W.; Methodology, Z.D. and Y.W.; Writing—Original Draft, D.L. and Y.W.; Writing—Review and Editing, K.L. and C.D.; Data Curation, Y.C. and J.Z.; Funding Acquisition, Y.W., K.L. and Z.D. All authors have read and agreed to the published version of the manuscript.

Funding: This study was funded by the National Natural Science Foundation of China (NNSFC) (52304052, 52304012) and the CNPC Science and Technology Project (2024DJ23).

Data Availability Statement: The original contributions presented in the study are included in the article, further inquiries can be directed to the corresponding author.

Acknowledgments: The authors acknowledge that this study was supported by the National Natural Science Foundation of China (52304052, 52304012) and the CNPC Science and Technology Project (2024DJ23).

Conflicts of Interest: Authors Dejiang Li, Ze Deng, Caiyuan Dong, Yan Chang and Jidong Zhang were employed by the company China National Petroleum Corporation (CNPC). The authors declare that this study received funding from NNSFC and CNPC. The funders CNPC and NNSFC were not involved in the study design, collection, analysis, interpretation of data, the writing of this article or the decision to submit it for publication.

References

1. Moore, T.A. Coalbed methane: A review. *Int. J. Coal Geol.* **2012**, *101*, 36–81. [CrossRef]
2. Bai, J.; Wang, H.; Ren, G.; Qiao, Y. Multiscale fracture characteristics of coal and their influence on fracture propagation. *Appl. Sci.* **2026**, *16*, 3214. [CrossRef]
3. Li, G.; Chen, R.; Wen, Z.; Zhang, J.; He, Z.; Feng, J.; Kang, H.; Meng, Q.; Ma, C.; Su, L. Global coal-rock gas resource potential and distribution. *Petrol. Explor. Dev.* **2026**, *53*, 14–26. [CrossRef]
4. Zhao, Z.; Xu, W.; Zhao, Z.; Yi, S.; Yang, W.; Zhang, Y.; Sun, Y.; Zhao, W.; Shi, Y.; Zhang, C.; et al. Geological characteristics and exploration breakthroughs of coal rock gas in Carboniferous Benxi Formation, Ordos Basin, NW China. *Petrol. Explor. Dev.* **2024**, *51*, 234–247. [CrossRef]
5. Yang, F.; Li, B.; Wang, K.J.; Wen, H.; Yang, R.Y.; Huang, Z.W. Extreme massive hydraulic fracturing in deep coalbed methane horizontal wells: A case study of the Linxing Block, eastern Ordos Basin, NW China. *Petrol. Explor. Dev.* **2024**, *51*, 389–398. [CrossRef]
6. Ouyang, W.; Huang, L.; Liu, J.; Zhang, M.; Sheng, G. Influence of complex lithology distribution on fracture propagation morphology in coalbed methane reservoir. *Appl. Sci.* **2024**, *14*, 11681. [CrossRef]
7. Butt, I.A.; Liang, W.; Rene, N.N.; Ali, A.; Yang, H.; Awan, F.U.R.; Shi, Q.-X.; Liu, X. Hierarchical controls on fracture sustainability in deep coal: Integrating stress-dependent permeability, microscale mechanics and ANN analysis. *Gas Sci. Eng.* **2026**, *152*, 205947. [CrossRef]
8. Burgoyne, M.; Shrivastava, R. A practical workflow for characterizing stress-dependent behaviour of coal from changes in well productivity. *J. Nat. Gas Sci. Eng.* **2016**, *33*, 1025–1045. [CrossRef]
9. McKee, C.R.; Bumb, A.C.; Koenig, R.A. Stress-dependent permeability and porosity of coal and other geologic formations. *SPE Form. Eval.* **1988**, *3*, 81–91. [CrossRef]
10. Palmer, I.; Mansoori, J. How permeability depends on stress and pore pressure in coalbeds: A new model. *SPE Reserv. Eval. Eng.* **1998**, *1*, 539–544. [CrossRef]
11. Shi, J.Q.; Durucan, S. Drawdown induced changes in permeability of coalbeds: A new interpretation of the reservoir response to primary recovery. *Transp. Porous Media* **2004**, *56*, 1–16. [CrossRef]
12. Shi, J.Q.; Durucan, S. A model for changes in coalbed permeability during primary and enhanced methane recovery. *SPE Reserv. Eval. Eng.* **2005**, *8*, 291–299. [CrossRef]

13. Cui, X.; Bustin, R.M. Volumetric strain associated with methane desorption and its impact on coalbed gas production from deep coal seams. *AAPG Bull.* **2005**, *89*, 1181–1202. [CrossRef]
14. Pan, Z.; Connell, L.D. A theoretical model for gas adsorption-induced coal swelling. *Int. J. Coal Geol.* **2007**, *69*, 243–252. [CrossRef]
15. Chen, M.; Masum, S.; Sadasivam, S.; Thomas, H. Modelling anisotropic adsorption-induced coal swelling and stress-dependent anisotropic permeability. *Int. J. Rock Mech. Min. Sci.* **2022**, *153*, 105107. [CrossRef]
16. Durucan, S.; Ahsan, M.; Shi, J.Q. Matrix shrinkage and swelling characteristics of European coals. *Energy Procedia* **2009**, *1*, 3055–3062. [CrossRef]
17. Battistutta, E.; van Hemert, P.; Lutynski, M.; Bruining, H.; Wolf, K.-H. Swelling and sorption experiments on methane, nitrogen and carbon dioxide on dry Selar Cornish coal. *Int. J. Coal Geol.* **2010**, *84*, 39–48. [CrossRef]
18. Lin, J.; Ren, T.; Wang, G.; Booth, P.; Nemcik, J. Experimental study of the adsorption-induced coal matrix swelling and its impact on ECBM. *J. Earth Sci.* **2017**, *28*, 917–925. [CrossRef]
19. Thararoop, P.; Karpyn, Z.T.; Ertekin, T. Development of a multi-mechanistic, dual-porosity, dual-permeability, numerical flow model for coalbed methane reservoirs. *J. Nat. Gas. Sci. Eng.* **2012**, *8*, 121–131. [CrossRef]
20. Sampath, K.; Perera, M.; Matthai, S.; Ranjith, P.; Dong-Yin, L. Modelling of fully-coupled CO2 diffusion and adsorption-induced coal matrix swelling. *Fuel* **2020**, *262*, 116486. [CrossRef]
21. Zhu, W.C.; Wei, C.H.; Liu, J.; Xu, T.; Elsworth, D. Impact of gas adsorption induced coal matrix damage on the evolution of coal permeability. *Rock Mech. Rock Eng.* **2013**, *46*, 1353–1366. [CrossRef]
22. Liu, P.; Fan, J.; Jiang, D. Laboratory measurement of permeability evolution behaviors induced by non-sorbing/sorbing gas depletion in coal using pulse-decay method. *Transp. Porous Media* **2021**, *139*, 595–613. [CrossRef]
23. Li, Y.; Wang, Y.; Wang, J.; Pan, Z. Variation in permeability during CO2-CH4 displacement in coal seams: Part 1—Experimental insights. *Fuel* **2020**, *263*, 116666. [CrossRef]
24. Tian, J.; Liu, J.; Elsworth, D.; Leong, Y.-K.; Li, W. An effective stress-dependent dual-fractal permeability model for coal considering multiple flow mechanisms. *Fuel* **2023**, *334*, 126800. [CrossRef]
25. Zhou, G.; Zhang, Z.; Wang, Y.; Tian, W.; Deng, Z.; Chen, H.; Wu, X.; Shen, J. The fracability evaluation of deep coal reservoirs in the Ordos Basin based on well logging and rock mechanics experiments. *Appl. Sci.* **2026**, *16*, 6084. [CrossRef]
26. Zhang, X.Y.; Wu, C.F.; Wang, Z.W. Experimental study of the effective stress coefficient for coal permeability with different water saturations. *J. Petrol. Sci. Eng.* **2019**, *182*, 106282. [CrossRef]
27. Li, J.; Li, B.; Pan, Z.; Wang, Z.; Yang, K.; Ren, C.; Xu, J. Coal permeability evolution under different water-bearing conditions. *Nat. Resour. Res.* **2020**, *29*, 2451–2465. [CrossRef]
28. Lei, J.; Meng, Z.; Tan, L.; Wang, Y.; Wu, D. Experimental study on stress-dependent permeability of coal samples with different salinities of water in coal. *Process Saf. Environ. Prot.* **2023**, *170*, 403–414. [CrossRef]
29. Yao, Y.B.; Ma, R.Y.; Sun, X.X. Mechanism of enhanced coalbed methane desorption regulated by fracturing fluid imbibition in deep coal seams. *Petrol. Explor. Dev.* **2025**, *52*, 1388–1400. [CrossRef]
30. Chen, D.; Pan, Z.; Liu, J.; Connell, L.D. An improved relative permeability model for coal reservoirs. *Int. J. Coal Geol.* **2013**, *109–110*, 45–57. [CrossRef]
31. Aghighi, M.A.; Cui, T.; Schöning, G.; Espinoza, D.N.; Pandey, S. Subsidence associated with dewatering and gas extraction from coal seams: Contribution of desorption-induced coal shrinkage. *J. Hydrol.* **2024**, *637*, 131355. [CrossRef]
32. Nainar, S.; Govindarajan, S.K. Semi-analytic analysis and optimization of stress-dependent permeability model for the coal bed methane gas reservoir. *Environ. Earth Sci.* **2021**, *80*, 272. [CrossRef]
33. Gray, I. Reservoir engineering in coal seams: Part 1—The physical process of gas storage and movement in coal seams. *SPE Reserv. Eng.* **1987**, *2*, 28–34. [CrossRef]
34. Ma, Q.; Harpalani, S. A simplified permeability model for coalbed methane reservoirs based on matchstick strain and constant volume theory. *Int. J. Coal Geol.* **2011**, *85*, 43–48. [CrossRef]
35. Liu, S.M.; Harpalani, S. A new theoretical approach to model sorption-induced coal shrinkage or swelling. *AAPG Bull.* **2013**, *97*, 1033–1049. [CrossRef]
36. Connell, L.D.; Lu, M.; Pan, Z.J. An analytical coal permeability model for tri-axial strain and stress conditions. *Int. J. Coal Geol.* **2010**, *84*, 103–114. [CrossRef]
37. Guo, X.; Jin, Y.; Miu, T.; Wei, S.; Xia, Y.; Tang, J. Investigation of the time-dependent and dynamic geomechanical behaviors induced by depressurization in natural gas hydrate-bearing sediments based on a poro-elasto-viscoplastic-dynamic model. *Int. J. Rock Mech. Min. Sci.* **2026**, *197*, 106357. [CrossRef]

Disclaimer/Publisher's Note: The statements, opinions and data contained in all publications are solely those of the individual author(s) and contributor(s) and not of MDPI and/or the editor(s). MDPI and/or the editor(s) disclaim responsibility for any injury to people or property resulting from any ideas, methods, instructions or products referred to in the content.